

# Size-Dependent Forced Vibration Analysis of Three Nonlocal Strain Gradient Beam Models with Surface Effects Subjected to Moving Harmonic Loads

K. Rajabi<sup>1,\*</sup>, Sh. Hosseini-Hashemi<sup>2</sup>, A.R. Nezamabadi<sup>3</sup>

<sup>1</sup>*Department of Mechanical Engineering, College of Engineering, Sanandaj Branch, Islamic Azad University, Sanandaj, Iran*

<sup>2</sup>*School of Mechanical Engineering, Iran University of Science and Technology, Tehran, Iran*

<sup>3</sup>*Department of Mechanical Engineering, Arak Branch, Islamic Azad University, Arak, Iran*

Received 6 September 2018; accepted 8 December 2018

## ABSTRACT

The forced vibration behaviors are examined for nonlocal strain gradient Nano beams with surface effects subjected to a moving harmonic load travelling with a constant velocity in terms of three beam models namely, the Euler-Bernoulli, Timoshenko and modified Timoshenko beam models. The modification for nonlocal strain gradient Timoshenko Nano beams is exerted to the constitutive equations by exclusion of the nonlocality in the shear constitutive relation. Some analytical closed-form solutions for three nonlocal strain gradient beam models with simply supported boundary conditions are derived by using the Galerkin discretization method in conjunction with the Laplace transform method. The effects of the three beam models, the nonlocal and material length scale parameters, the velocity and excitation frequency of the moving harmonic load on the dynamic behaviors of Nano beams are discussed in some detail. Specifically, the critical velocities are examined in some detail. Numerical results have shown that the aforementioned parameters are very important factors for determining the dynamic behavior of the Nano beams accurately.

© 2019 IAU, Arak Branch. All rights reserved.

**Keywords :** Nonlocal strain gradient elasticity theory; Euler-Bernoulli beam model; Timoshenko beam model; Moving harmonic load; Analytical solution.

## 1 INTRODUCTION

**A**FTER discovery of carbon nanotubes (CNTs), many theoretical and experimental efforts have been conducted to investigate their mechanical behavior. CNTs have extremely high strength, low mass density, nearly perfect geometrical structure and linear elastic behavior for longitudinal strain lower than 12% [1]. These extraordinary properties of CNTs provide them in many applications in nanotechnology, Nano biology, optic, electronic, and as well as in medical fields [1]. Among aforementioned fields of applications, one possibly use of them is as new transporter systems for the delivery of drugs. In such a case, one encounters the problem of

\*Corresponding author. Tel.: +98 9188781579.  
E-mail address: [rajabi.kaveh@gmail.com](mailto:rajabi.kaveh@gmail.com) (K. Rajabi).

interaction between CNTs and moving nanoscale objects [1]. Nowadays, the traditional idea of making a molecular machine has been met in the real world of nanotechnology. These small-sized machines are working based on electrical voltage, chemical conversion, external light or temperature [2-7]. Being able to move molecules on a surface, they can also be used as a transport device of several atoms [6]. In all these applications, one encounters the problem of nanostructure–moving nanoparticle interaction, mostly because of the mass weights of the nanoparticles and the friction between the surfaces of the nanoparticle and the nanotube structure [1, 7-10]. Dynamic analysis of CNTs under action of moving nanoparticles has been addressed in the literature, *e.g.*, Kiani [7, 8, 10, 11] has investigated the problems of interaction between CNTs and moving nanoparticles analytically using various nonlocal continuum beam theories and Ghorbanpour Arani et al. [12] have presented the vibration of a single-walled Boron Nitride nanotube (SWBNNT) under action of a moving nanoparticle using nonlocal Euler-Bernoulli beam theory. As one knows, conducting experimental tests at nano-scales are much harder than those at macro-scales. Furthermore, molecular dynamics (MD) and quantum mechanics based simulations are computationally expensive [8, 9, 13]. To overcome these difficulties arising in atomistic methods, the continuum mechanics formulations have been employed by many researchers. The governing differential equations of classical continuum theories may be derived from the finite difference equations in terms of lattice dynamics by using some series expansions (*e.g.*, the Taylor expansion or Pade' approximants) and considering the first-order truncation. Therefore, due to the first-order truncation, the classical continuum mechanics are restricted to long-wave and low-frequency dynamics, and hence can only be accurate for phenomena with an internal characteristic length (*e.g.*, carbon-carbon bond length) much smaller than macroscopic characteristic lengths. For NEMS, the internal characteristic length is comparable with the geometric characteristic lengths. As a result, as experimental findings have shown, that in nanoscale phenomena the size effects have great influences on the physical properties and mechanical responses of NEMS [14, 15], which do not show an agreement with the predicted results of classical continuum models. In classical continuum mechanics, all standard constitutive models which simulate the mechanical behavior of solids have no size-dependent material parameters. In this context, the stress at a given point uniquely depends on the current values and possibly the previous history of deformation and temperature at that point only [16, 17]. There are different manners to refine the classical continuum models from the atomistic view to the constitutive laws such that their range of applicability can be extended to analyze the size-dependent problems accounting for smaller internal characteristic lengths.

One possibility is to modify the constitutive law of classical continuum models from local elasticity to nonlocal elasticity. In the case of nonlocal constitutive laws, finite microscopic nonlocal parameters are introduced to account for, for instance, the length between neighboring atoms in lattice structures. Generally speaking, there are two enriched nonlocal continuum mechanics formulations: weakly nonlocal (gradient type) and strongly nonlocal (integral type) formulations [17, 18]. In a gradient-type nonlocal model, the constitutive law is enriched with the first or higher gradients of strain tensor. An obvious characteristic of this enriched model is the presence of one or more material parameters in constitutive relations (*e.g.*, [19-21]). Also, it is worth to notice that in the gradient-type or weakly nonlocal formulations constitutive law in a typical point is written in an immediate vicinity of that point. On the other hand, in strongly nonlocal model the constitutive law at a typical point involves weighted averages of a state variable over a certain neighborhood of that point (*e.g.*, [22-25]). Previous studies revealed that the Eringen's nonlocal elastic models could only account for stiffness-softening phenomena with increasing nonlocal parameter. Another possibility is to derive the continuum equation by accounting for second- or higher-order terms in the series expansions of the finite difference equations of lattice dynamics or discrete media, which leads to the so-called strain gradient theories with different orders [26] (the classical continuum theories can be viewed as the lowest-order strain gradient theory). The stiffness enhancement effect noticed from experimental observations can be reasonably explained by these strain gradient theories.

Recently, experimental findings have shown that both stiffness-softening and stiffness-enhancement phenomena can be observed, depending on the microstructures, at nanoscale [27, 28]. As discussed above, the material length scales presented in Eringen's nonlocal theory and strain gradient theories describe two entirely different physical characteristics of materials and structures at nanoscale. There is a need to bring both theories into a single theory so that the true effect of two material length scales can be captured correctly. To this end, recently a theory is developed to assess the two size-dependent material characteristic parameters by combining the strain gradient theory with Eringen's nonlocal elasticity theory [29]. The theory is called nonlocal strain gradient theory and it has been applied in various nanoscale problems (*e.g.*, [30-39]). Many researchers have recently examined the scaling effects on the mechanical behaviors of rod [34, 40], shaft [41, 42], beams [43, 44] and plates [45], and showed that both stiffness-softening or stiffness-enhancement phenomenon depends on the given values of the nonlocal parameter and the material length scale parameter. These nonlocal strain gradient models may be simplest model to account for both the stiffness-softening and stiffness-enhancement effects, which qualitatively explain the

phenomena observed in experimental results [27, 28]. It is concluded that the nonlocal strain gradient models can yield good trade-off between accuracy and computational complexity.

To account for both the stiffness-softening and stiffness-enhancement effects on the forced vibration of Nano beams subjected to moving harmonic loads, the forced vibration of Nano beams subjected to moving harmonic loads will be studied in the frameworks of the nonlocal strain gradient elasticity theory. Furthermore, the surface effects can play a significant role in the forced vibration behaviors of Nano beams owing to the very significant surface-to-volume ratio of Nano beams [46-54]. Hence in this study, we have carried out the problem of forced vibration of size-dependent Euler-Bernoulli and Timoshenko Nano beams with surface effects acted upon by a moving harmonic load in the frameworks of the nonlocal strain gradient elasticity theory. In this regard, analytical solutions have been presented. The schematic of a SWCNT is shown in Fig.1. The length, diameter and the thickness of the SWCNT are denoted by  $L$ ,  $d$  and  $h$  respectively. A moving harmonic load enters into the SWCNT from the left boundary and leaves it from the right boundary. It travels with a constant speed, say  $v$ .

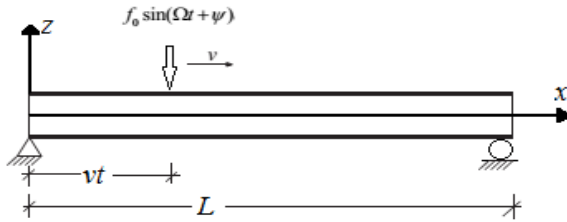


**Fig.1**  
Schematic of a SWCNT subjected to a moving harmonic load.

## 2 EQUATIONS OF MOTION

### 2.1 Nonlocal strain gradient theory

Lim et al. [29] proposed a nonlocal strain gradient elasticity theory which considers higher-order stress gradients and strain gradient nonlocality. By employing the constitutive relation within the thermodynamic framework, they obtained the equilibrium equations and all related boundary conditions via the variational approach. This theory has generalized Eringen’s nonlocal elasticity theory by introducing a higher-order strain tensor with nonlocality into the stored energy function. The developed theory is distinctive because Eringen’s nonlocal elasticity does not include nonlocality of higher-order stresses while common strain gradient theories only consider local higher-order strain gradients without nonlocal effects in global sense [29, 34].

In the nonlocal strain gradient theory, a new stress tensor is introduced:

$$\mathbf{t} = \boldsymbol{\sigma} - \nabla \cdot \boldsymbol{\sigma}^{(1)} \tag{1}$$

where  $\mathbf{t}$  is the total stress tensor,  $\boldsymbol{\sigma}$  is the classical nonlocal stress tensor and  $\boldsymbol{\sigma}^{(1)}$  is a higher-order nonlocal stress tensor defined as:

$$\boldsymbol{\sigma} = \int_V \alpha_0(\mathbf{x}', \mathbf{x}, e_0 a) \mathbf{C} : \boldsymbol{\varepsilon}' dV' \tag{2}$$

$$\boldsymbol{\sigma}^{(1)} = l^2 \int_V \alpha_1(\mathbf{x}', \mathbf{x}, e_1 a) \mathbf{C} : \nabla \boldsymbol{\varepsilon}' dV' \tag{3}$$

where  $l$  is a gradient material characteristic parameter, termed henceforth the gradient parameter (for the sake of brevity), introduced to determine the significance of higher-order strain gradient field,  $\alpha_1(\mathbf{x}', \mathbf{x}, e_1 a)$  is an additional attenuation kernel function introduced to describe the nonlocal effect of the first-order strain gradient field, and  $e_1$  is the related material constant [29].

### 2.2 Euler-Bernoulli beam model

Within the framework of Euler-Bernoulli beam model, the integral constitutive equation is written as:

$$t_{xx} = \sigma_{xx} - \sigma_{xx,x}^{(1)} \quad (4)$$

$$\sigma_{xx} = \int_0^L E \alpha_0(x, x', e_0 a) \varepsilon'_{xx}(x') dx' \quad (5)$$

$$\sigma_{xx}^{(1)} = l^2 \int_0^L E \alpha_1(x, x', e_1 a) \varepsilon'_{xx,x}(x') dx' \quad (6)$$

where  $L$  and  $E$  are the length and Young's modulus of the Nano beam in order and a comma before a variable denotes differentiation with respect to that variable. By assuming that the attenuation kernels satisfy the conditions of Eringen's nonlocal elasticity [17, 24, 29], the differential counterpart of Eq. (4) is written as:

$$(1 - (e_1 a)^2 \nabla^2)(1 - (e_0 a)^2 \nabla^2)t_{xx} = E(1 - (e_1 a)^2 \nabla^2)\varepsilon_{xx} - El^2(1 - (e_0 a)^2 \nabla^2)\nabla^2\varepsilon_{xx} \quad (7)$$

where  $\nabla^2 = d^2/dx^2$  is the one-dimensional Laplacian operator (as usual, the size-dependent behavior is assumed to be neglected in the radius direction for a Nano beam-type structure). Eq. (7) is the nonlocal strain gradient differential constitutive relation for an Euler-Bernoulli beam. It contains three material length scales, one accounts for the size effect induced by strain gradients (i.e.,  $l^2$ ), one for the lower-order nonlocal stress (i.e.,  $e_0$ ) and the third one for the higher-order nonlocal stress (i.e.,  $e_1$ ).

By assuming  $e_0 = e_1 = e$  and retaining terms of order  $O(\nabla^2)$ , the reduced version of the general constitutive relation (7) can be obtained as:

$$(1 - (ea)^2 \nabla^2)t_{xx} = E(1 - l^2 \nabla^2)\varepsilon_{xx} \quad (8)$$

Using Hamilton's principle, the governing equation of an Euler-Bernoulli Nano beam can be obtained as:

$$EI(1 - l^2 \nabla^2)w_{,xxxx} + \rho A(1 - (ea)^2 \nabla^2)w_{,tt} = (1 - (ea)^2 \nabla^2)f(x, t) \quad (9)$$

where  $A$  is the cross sectional area,  $I$  is the second moment of inertia and  $\rho$  is the mass density. In above equation,  $f(x, t)$  is the external load on the Nano beam which in the case of a moving force is defined as:

$$f(x, t) = P(t)\delta(x - vt) \quad (10)$$

where  $P(t)$  is the amplitude of the moving load,  $v$  is the constant velocity of the moving load and  $\delta(\bullet)$  is Dirac delta function.

The associated boundary conditions are written as:

$$\begin{aligned} M_{,x} &= 0 \quad \text{or} \quad w = 0 \\ M &= 0 \quad \text{or} \quad w_{,x} = 0 \\ M^{(1)} &= 0 \quad \text{or} \quad w_{,xx} = 0 \end{aligned} \quad (11)$$

where  $M = \iint_A z t_{xx} dA$ , is the total bending moment in a typical cross section of the Nano beam ;  $M^{(1)} = \iint z \sigma_{xx}^{(1)} dA$ , is the bending moment due to higher-order stress component. From Eq. (9) it is seen that by setting  $l=0$ , the governing equation of a classical nonlocal Nano beam will be recovered.

It is a well-known fact that at nanoscale, due to increasing ratio of the surface area to bulk, the surface stress will play a prominent role. This motivates the researchers to take it into consideration in their relevant studies (e.g., [46-

54]). In this study to address the influence of the residual surface stress on the dynamic deflection of the Euler-Bernoulli Nano beam s, according to the Laplace-Young equation, the distributed transverse load is thus written as [46, 48]:

$$q(x, t) = Hw_{,xx} \quad (12)$$

where  $H$  is a constant determined by the shape of the cross section and also the residual surface tension as given by [46]:

$$H = \begin{cases} 2\tau^0 b, & (\text{rectangle}) \\ 2\tau^0 d, & (\text{circular}) \end{cases} \quad (13)$$

where  $\tau^0$ ,  $b$  and  $d$  are the residual surface tension, width and diameter of the Nano beam s. The bending rigidity of the Nano beam is modified to account for the surface elasticity [46]:

$$\begin{aligned} (EI)^* &= EI + \frac{1}{2}E_s b h^2 + \frac{1}{6}E_s h^3, & (\text{Rec.}) \\ (EI)^* &= EI + \frac{\pi}{8}E_s d^3, & (\text{Circular}) \end{aligned} \quad (14)$$

where  $(EI)^*$  and  $E_s$  are the effective bending rigidity and surface elastic modulus respectively. Finally Eq. (9) is modified to account for the surface elasticity as:

$$(EI)^*(1-l^2\nabla^2)w_{,xxxx} + \rho A(1-(ea)^2\nabla^2)w_{,tt} - H(1-(ea)^2\nabla^2)w_{,xx} = (1-(ea)^2\nabla^2)f(x, t) \quad (15)$$

By introducing the following non-dimensional variables to Eq. (15), one can obtain the normalized version of the governing equation of motion as given in Eq. (17).

$$X = \frac{x}{L}, W = \frac{w}{L}, \tau = \frac{t}{T} \quad (16)$$

$$(1-\lambda^2\bar{\nabla}^2)W_{,XXXX} - \bar{H}(1-\mu^2\bar{\nabla}^2)W_{,XX} + (1-\mu^2\bar{\nabla}^2)W_{,\tau\tau} = (1-\mu^2\bar{\nabla}^2)\bar{f}(X, \tau) \quad (17)$$

where the following parameters have been defined:

$$\bar{\nabla}^2 = \frac{\partial^2}{\partial X^2}, \lambda = \frac{l}{L}, \mu = \frac{ea}{L}, \bar{H} = \frac{H L^2}{(EI)^*}, \bar{f}(X, \tau) = \frac{L^3 f(LX, T\tau)}{(EI)^*}, T = L^2 \sqrt{\frac{\rho A}{(EI)^*}} \quad (18)$$

### 2.3 Timoshenko beam model

Two nonlocal Timoshenko beam theories are available in the literature. In both theories, the scale effect is well modeled in the constitutive equation of axial stress and strain [55, 56]. Wang and Wang [56] have proposed that there is no necessity to include the nonlocality in the shear constitutive relation. Arash and Wang [55] compared the fundamental resonant frequency of single-walled carbon nanotubes (SWCNTs) obtained from the two Timoshenko beam models and shown that there is a negligible discrepancy between the predicted resonant frequencies of two beam models. However, this comparison has not been done for the nonlocal strain gradient elasticity theory. Hence in this study, we will adopt the same strategy to propose a modified nonlocal strain gradient Timoshenko beam model and compare the new beam model with the conventional one. By using the extended Hamilton's principle, the general governing equations of motion of a nonlocal strain gradient Timoshenko Nano beam can be derived as (cf. Ref. [36]):

$$\rho I \left(1 - (ea)^2 \nabla^2\right) \varphi_{,tt} - \left(1 - l^2 \nabla^2\right) \left[ kAG (w_{,x} - \varphi) + EI \varphi_{,xx} \right] = 0 \quad (19)$$

$$kAG \left(1 - l^2 \nabla^2\right) (w_{,xx} - \varphi_{,x}) - \rho A \left(1 - (ea)^2 \nabla^2\right) w_{,tt} + \left(1 - (ea)^2 \nabla^2\right) f(x, t) = 0 \quad (20)$$

where  $k$ ,  $G$  and  $\varphi$  are the shear correction factor, shear modulus and rotation of the cross-section of the Nano beam respectively. It has to be noted here that in this model, the nonlocality has been considered in the shear constitutive relation. The following classical boundary equations are given:

$$\begin{aligned} M &= 0 \text{ or } \varphi = 0 \\ Q_z &= 0 \text{ or } w = 0 \end{aligned} \quad (21)$$

and the non-classical boundary conditions:

$$\begin{aligned} M^{(1)} &= 0 \text{ or } \varphi_{,x} = 0 \\ Q_z^{(1)} &= 0 \text{ or } (w_{,x} - \varphi) = 0 \end{aligned} \quad (22)$$

where  $(Q_z, Q_z^{(1)}) = k \iint_A (t_{xz}, \tau_{xz}^{(1)}) dA$  are the shear resultants. Similar to the Euler-Bernoulli model, we modify Eqs. (19) -(20) to account for the effect of surface elasticity on the dynamic response of size-dependent Timoshenko Nano beam s as:

$$\rho I \left(1 - (ea)^2 \nabla^2\right) \varphi_{,tt} - \left(1 - l^2 \nabla^2\right) \left[ kAG (w_{,x} - \varphi) + (EI)^* \varphi_{,xx} \right] = 0 \quad (23)$$

$$kAG \left(1 - l^2 \nabla^2\right) (w_{,xx} - \varphi_{,x}) - \rho A \left(1 - (ea)^2 \nabla^2\right) w_{,tt} + H \left(1 - (ea)^2 \nabla^2\right) w_{,xx} = \left(-1 + (ea)^2 \nabla^2\right) f(x, t) \quad (24)$$

By introducing Eq. (18) to the above equations, one can obtain the following normalized governing equations of motion of size-dependent Timoshenko Nano beam s as:

$$\left(1 - \mu^2 \bar{\nabla}^2\right) \varphi_{,\tau\tau} - \bar{k} \left(1 - \lambda^2 \bar{\nabla}^2\right) (W_{,x} - \varphi) - \bar{A} \left(1 - \lambda^2 \bar{\nabla}^2\right) \varphi_{,xx} = 0 \quad (25)$$

$$\left(1 - \lambda^2 \bar{\nabla}^2\right) (W_{,xx} - \varphi_{,x}) - \bar{k} \left(1 - \mu^2 \bar{\nabla}^2\right) W_{,\tau\tau} + \bar{H} \left(1 - \mu^2 \bar{\nabla}^2\right) W_{,xx} = \left(-1 + \mu^2 \bar{\nabla}^2\right) \bar{f}(X, \tau) \quad (26)$$

where the following parameters have been defined:

$$\bar{k} = \frac{kA^2 GL^4}{I(EI)^*}, \bar{A} = \frac{AL^2}{I}, \bar{k} = \frac{(EI)^*}{kAGL^2}, \bar{H} = \frac{H}{kAG}, \bar{f}(X, \tau) = \frac{Lf(LX, T\tau)}{kAG} \quad (27)$$

Now, we propose a modification to the presented nonlocal strain gradient Timoshenko beam model. To do so, the nonlocality has to be excluded in the shear constitutive relation:

$$Q_z^{nl} = Q_z^l = kAG(w_{,x} - \varphi) \quad (28)$$

where it has been assumed that the local and nonlocal shear resultants are the same. Using the above relation, the governing equations of the modified nonlocal strain gradient Timoshenko beam model with the surface effects can be derived as:

$$\rho I \left(1 - (ea)^2 \nabla^2\right) \varphi_{,tt} + \rho A (ea)^2 w_{,ttx} - kAG (w_{,x} - \varphi) - (EI)^* \left(1 - l^2 \nabla^2\right) \varphi_{,xx} - (ea)^2 (f_{,x} + Hw_{,xxx}) = 0 \tag{29}$$

$$\rho A w_{,tt} - kAG (w_{,xx} - \varphi_{,x}) - Hw_{,xx} - f(x, t) = 0 \tag{30}$$

As seen from the above equations, by setting  $l = ea = 0$ , the well-known equations of motion for classical Timoshenko beams will be recovered.

### 3 METHOD OF SOLUTION

Numerical solutions are generally used for analyzing various engineering problems [57, 58]. Despite this fact, they have their own limitations concerning accuracy, stability, and convergence. On the other hand, analytical or even semi-analytical solutions are more appealing to researchers because of various advantages such as less computational time, ease of parametric study, and providing a deeper physical insight into the underlying problem. Some researchers have presented analytical solutions for the forced vibration analysis of Nano beam s subjected to moving loads. For instant, Kiani and Mehri [7] have employed the Galerkin method and the Laplace transform method to obtain analytical solutions, regarding to single-walled carbon nanotubes (SWCNTs), for various nonlocal beam models acted upon by a concentrated moving force. Kiani [8, 11] have employed the same methodology to obtain analytical solutions, regarding to double-walled carbon nanotubes (DWCNTs), for various nonlocal beam models acted upon by a concentrated moving force. Hosseini and Rahmani [32] have analyzed the axial and transverse dynamic response of a functionally graded Nano beam under a concentrated moving force. Analytical solutions have been presented by a combination of the Galerkin and Laplace transform methods.

In this study, by using the Galerkin discretization method in conjunction with the Laplace transform method, some analytical solutions for the three nonlocal strain gradient beams models namely, the Euler-Bernoulli, Timoshenko and modified Timoshenko beam models with simply supported boundary conditions will be derived.

We consider a concentrated moving harmonic load on simply supported Nano beam s. The load moves in the axial direction of the Nano beam s with a constant velocity, thus the load  $f(x, t)$ , is written as:

$$f(x, t) = f_0 \sin(\Omega t + \psi) \delta(x - vt) \tag{31}$$

where  $f_0$ ,  $\Omega$  and  $\psi$  are the amplitude, the excitation frequency and the phase angle of the moving harmonic load respectively.

#### 3.1 Euler-Bernoulli Nano beam s

For simply supported boundary conditions, we employ the Galerkin method for discretizing the governing equation of motion. To this end, the flexural deflection of the Nano beam is assumed to be:

$$W(X, \tau) = \sum_{i=1}^N \sin(i \pi X) q_i(\tau) \tag{32}$$

where the sine functions satisfy the simply supported boundary conditions and  $q_i(\tau)$  are the unknown generalized functions. Introduce Eq. (32) to Eq.(17), then multiply both sides of the resulted equation with  $\sin(n\pi X)$ ,  $n = 1, 2, \dots, N$ , and integrate it over the domain to obtain the following ordinary differential equation in terms of the  $n$ th generalized function:

$$(1 + \mu^2 \gamma_n^2) q_{n,\tau\tau} + (\lambda^2 \gamma_n^6 + \gamma_n^4 + \bar{H} \gamma_n^2 (1 + \mu^2 \gamma_n^2)) q_n = \frac{2f_0 L^2}{(EI)^*} (1 + \mu^2 \gamma_n^2) \sin(\Omega T \tau + \psi) \sin\left(\frac{\gamma_n v T \tau}{L}\right) \tag{33}$$

where  $\gamma_n = n\pi$ . Eq. (33) can be then simplified as given below:

$$q_{n,\tau\tau} + \omega_n^2 q_n = \frac{2L^2 f_0}{(EI)^*} \sin(\Omega T \tau + \psi) \sin\left(\frac{\gamma_n v T \tau}{L}\right), \quad n = 1, 2, \dots, N \quad (34)$$

where

$$\omega_n = \sqrt{\frac{\lambda^2 \gamma_n^6 + \gamma_n^4 + \bar{H} \gamma_n^2 (1 + \mu^2 \gamma_n^2)}{1 + \mu^2 \gamma_n^2}} \quad (35)$$

To complete the solution process, Eq. (34) should be solved by an appropriate method. In this study, we have employed the Laplace transform method for solving Eq. (34) in time domain. In order to be able to apply the Laplace transform to Eq. (34), it is firstly necessary to expand the external excitation as follows:

$$\begin{aligned} \sin(\Omega T \tau + \psi) \sin(\lambda_n \tau) &= \cos(\psi) \sin(\Omega T \tau) \sin(\lambda_n \tau) + \sin(\psi) \cos(\Omega T \tau) \sin(\lambda_n \tau) = \\ &= \frac{\cos(\psi)}{2} (\cos(\alpha_n \tau) - \cos(\beta_n \tau)) + \frac{\sin(\psi)}{2} (\sin(\beta_n \tau) - \sin(\alpha_n \tau)) \end{aligned} \quad (36)$$

where  $\lambda_n = n\pi v T / L$ ,  $\alpha_n = \Omega T - \lambda_n$  and  $\beta_n = \Omega T + \lambda_n$ . Using the above relations, Eq. (34) is rewritten as:

$$q_{n,\tau\tau} + \omega_n^2 q_n = f_1 (\cos(\alpha_n \tau) - \cos(\beta_n \tau)) + f_2 (\sin(\beta_n \tau) - \sin(\alpha_n \tau)), \quad n = 1, 2, \dots, N \quad (37)$$

where  $f_1 = L^2 f_0 \cos(\psi) / (EI)^*$  and  $f_2 = L^2 f_0 \sin(\psi) / (EI)^*$ . Applying the Laplace transform to Eq. (37) with zero initial conditions yields:

$$\bar{Q}_n(s) = \frac{f_1 s - \alpha_n f_2}{(s^2 + \omega_n^2)(s^2 + \alpha_n^2)} + \frac{-f_1 s + \beta_n f_2}{(s^2 + \omega_n^2)(s^2 + \beta_n^2)} \quad (38)$$

where  $s$  is the independent variable in Laplace domain and the over-bar denotes Laplace transform of a function. By using the Inverse Laplace transform, Eq. (38) can be obtained as:

$$q_n(\tau) = c_{\alpha n} \cos(\alpha_n \tau) + s_{\alpha n} \sin(\alpha_n \tau) + c_{\beta n} \cos(\beta_n \tau) + s_{\beta n} \sin(\beta_n \tau) + c_{\omega n} \cos(\omega_n \tau) + s_{\omega n} \sin(\omega_n \tau) \quad (39)$$

The constants appearing in above equation are summarized in Appendix A. Finally, the dynamic transverse deflection of a simply supported nanoscale beam acted upon by a moving harmonic load based on the Euler-Bernoulli beam model with surface effects is obtained, during the course of excitation (or the first phase of vibration), as given below:

$$W(X, \tau) = \sum_{n=1}^N \left[ c_{\alpha n} \cos(\alpha_n \tau) + s_{\alpha n} \sin(\alpha_n \tau) + c_{\beta n} \cos(\beta_n \tau) + s_{\beta n} \sin(\beta_n \tau) + c_{\omega n} \cos(\omega_n \tau) + s_{\omega n} \sin(\omega_n \tau) \right] \sin(n\pi X) \quad (40)$$

It is worth to mention that the Nano beam will experience free vibration when the moving harmonic load departs the right edge of the Nano beam. The dynamic response of the Nano beam, during the course of free vibration, can be obtained by using the Laplace transform method. To do so, one should first remove the excitation force from the right hand side of Eq. (37), then applies the Laplace transform to the obtained equation. The initial conditions of the free vibration (or the second phase of vibration) can be calculated from Eq. (40) at the associated dimensionless time  $\tau_f = \sqrt{(EI)^* / (\rho A v^2 L^2)}$ ; where  $\tau_f$  stands for the time duration of the first phase of motion.

The critical velocity of particle-conveying beams/tubes (also known as the divergence velocity) is of fundamental interest, and it implies that the particle-conveying beams may cause a bifurcation instability by buckling. When the particle velocity is beyond the critical velocity, the forced vibration deflections may produce

large deformations and no longer satisfy the requirement of linear theory. Under that case, the forced vibration behaviors have to be answered by using nonlinear beam models. For this reason, it is important to predict the critical velocity accurately.

In the following, we deal with the interesting issue of finding the critical velocities. As one can see from the relations given in Eq. (A.1) (Appendix A), two special cases can be deduced:

$$\begin{aligned} \omega_n = \beta_n \Rightarrow v_{ncr\beta} &= \frac{L}{n\pi} \left( \Omega_{ncr}^E - \Omega \right), \text{ for } \Omega < \Omega_{ncr}^E = \frac{\omega_n}{T}, \\ \omega_n = \alpha_n \Rightarrow v_{ncr\alpha} &= \frac{L}{n\pi} \left( \Omega - \Omega_{ncr}^E \right), \text{ for } \Omega > \Omega_{ncr}^E \end{aligned} \tag{41}$$

where  $T$  and  $\omega_n$  are given in Eq. (18) and Eq. (35) respectively. For these special cases, the denominators in relations given in Eq. (A.1) take zero values. Note that the letter  $n$  in the subscripts implies that for each values of  $n$  there is a critical velocity parameter. Introducing Eqs. (18) and (35) to Eq. (46) yields the following explicit forms for the critical velocities:

$$\begin{aligned} v_{ncr\beta}^E &= \frac{L}{n\pi} \left( \sqrt{\frac{(EI)^* \left( \lambda^2 \gamma_n^6 + \gamma_n^4 + \bar{H} \gamma_n^2 (1 + \mu^2 \gamma_n^2) \right)}{\rho AL^4 (1 + \mu^2 \gamma_n^2)}} - \Omega \right) \text{ for } \Omega < \sqrt{\frac{(EI)^* \left( \lambda^2 \gamma_n^6 + \gamma_n^4 + \bar{H} \gamma_n^2 (1 + \mu^2 \gamma_n^2) \right)}{\rho AL^4 (1 + \mu^2 \gamma_n^2)}}, \\ v_{ncr\alpha}^E &= \frac{L}{n\pi} \left( \Omega - \sqrt{\frac{(EI)^* \left( \lambda^2 \gamma_n^6 + \gamma_n^4 + \bar{H} \gamma_n^2 (1 + \mu^2 \gamma_n^2) \right)}{\rho AL^4 (1 + \mu^2 \gamma_n^2)}} \right) \text{ for } \Omega > \sqrt{\frac{(EI)^* \left( \lambda^2 \gamma_n^6 + \gamma_n^4 + \bar{H} \gamma_n^2 (1 + \mu^2 \gamma_n^2) \right)}{\rho AL^4 (1 + \mu^2 \gamma_n^2)}} \end{aligned} \tag{42}$$

where the superscript  $E$  stands for Euler-Bernoulli beam model. From above equations it is cleared that the critical velocities depend on the various parameters which among them, in our opinion, the excitation frequency of the moving harmonic load should be emphasized. Specifically, three immediate observations are summarized in the following:

- First, for the cases of  $\Omega < \Omega_{ncr}^E, n = 1, 2, \dots$ , increasing/decreasing the excitation frequency leads to a(n) decrease/increase in the values of the critical velocities,
- Second, for the cases of  $\Omega > \Omega_{ncr}^E, n = 1, 2, \dots$ , increasing/decreasing the excitation frequency leads to an/a increase/decrease in the values of the critical velocities,
- Third, when the nonlocal parameter is equal to the material characteristic length scale parameter (i.e.,  $\mu = l$ ), the response of the Nano beam predicted by the nonlocal strain gradient elasticity coincides with that of classical elasticity.

For each case of the above critical velocities, one should reconstruct Eq. (38) to capture the dynamic deflection of the Euler-Bernoulli Nano beam, as given below:

$$\begin{aligned} \bar{Q}_n(s) &= \frac{f_{n1}s - \alpha_n f_{n2}}{(s^2 + \omega_n^2)(s^2 + \alpha_n^2)} - \frac{f_{n1}s - \omega_n f_{n2}}{(s^2 + \omega_n^2)^2} \text{ for } v = v_{ncr\beta}^E, \\ \bar{Q}_n(s) &= \frac{f_{n1}s - \omega_n f_{n2}}{(s^2 + \omega_n^2)^2} - \frac{f_{n1}s - \beta_n f_{n2}}{(s^2 + \omega_n^2)(s^2 + \beta_n^2)} \text{ for } v = v_{ncr\alpha}^E \end{aligned} \tag{43}$$

The inverse Laplace transform of the above equations are given in the following:

$$\begin{aligned} W^E(X, \tau) &= \sum_{n=1}^N \left[ a_{ncr\beta} \cos(\alpha_n \tau) + b_{ncr\beta} \sin(\alpha_n \tau) + (c_{ncr\beta} + d_{ncr\beta} \tau) \cos(\omega_n \tau) + (e_{ncr\beta} + f_{ncr\beta} \tau) \sin(\omega_n \tau) \right] \sin(n\pi X), v = v_{ncr\beta}^E, \\ W^E(X, \tau) &= \sum_{n=1}^N \left[ a_{ncr\alpha} \cos(\beta_n \tau) + b_{ncr\alpha} \sin(\beta_n \tau) + (c_{ncr\alpha} + d_{ncr\alpha} \tau) \cos(\omega_n \tau) + (e_{ncr\alpha} + f_{ncr\alpha} \tau) \sin(\omega_n \tau) \right] \sin(n\pi X), v = v_{ncr\alpha}^E \end{aligned} \tag{44}$$

The constants appearing in above relations are summarized in Appendix A (Eq.(A.7)).

### 3.2 Timoshenko Nano beam s

In this subsection, we will solve the normalized governing equations of motion of a size-dependent Timoshenko Nano beam acted upon by a moving harmonic load using the same procedure as presented in the previous subsection. Again, we restrict our attention to the simply supported boundary conditions only. The present method of solution can be implemented for other boundary conditions by a straightforward manner. The normalized simply supported boundary conditions are by:

$$\begin{aligned} W(0, \tau) = W(1, \tau) = 0, \\ \varphi_{,X}(0, \tau) = \varphi_{,X}(1, \tau) = 0 \end{aligned} \quad (45)$$

To satisfy the given boundary conditions, the displacement field is given as:

$$W(X, \tau) = \sum_{n=1}^N \sin(n\pi X) p_n(\tau) \quad (46)$$

$$\varphi(X, \tau) = \sum_{n=1}^N \cos(n\pi X) q_n(\tau) \quad (47)$$

Now, first, apply the Galerkin method to Eqs. (25) -(26) to obtain the following set of coupled ordinary differential equations:

$$q_{n,\tau\tau} + c_{1n} q_n + d_{1n} p_n = 0 \quad (48)$$

$$p_{n,\tau\tau} + c_{2n} p_n + d_{2n} q_n = f_n \quad (49)$$

In which, for the sake of brevity, the following parameters are introduced:

$$\begin{aligned} c_{1n} &= \frac{(1 + \lambda^2 \gamma_n^2)(\bar{k} + \bar{A} \gamma_n^2)}{1 + \mu^2 \gamma_n^2}, d_{1n} = \frac{-\bar{k} \gamma_n (1 + \lambda^2 \gamma_n^2)}{1 + \mu^2 \gamma_n^2}, c_{2n} = \frac{\gamma_n^2 (1 + \lambda^2 \gamma_n^2) + \bar{H} \gamma_n^2 (1 + \mu^2 \gamma_n^2)}{\bar{k} (1 + \mu^2 \gamma_n^2)}, \\ d_{2n} &= \frac{-\gamma_n (1 + \lambda^2 \gamma_n^2)}{\bar{k} (1 + \mu^2 \gamma_n^2)}, f_n = \frac{2f_0}{kAGk} \sin(\Omega T \tau + \psi) \sin\left(\frac{\gamma_n v T \tau}{L}\right) \end{aligned} \quad (50)$$

Now one may apply the Laplace Transform to Eqs. (48) -(49) to yield the following relations:

$$\bar{Q}_n = \frac{-f_0 d_{1n}}{kAGk (s^2 + s_{1n}^2)(s^2 + s_{2n}^2)} \left[ \frac{\cos(\psi)s - \sin(\psi)\alpha_n}{s^2 + \alpha_n^2} + \frac{-\cos(\psi)s + \sin(\psi)\beta_n}{s^2 + \beta_n^2} \right] \quad (51)$$

$$\bar{P}_n = \frac{f_0 (s^2 + c_{1n})}{kAGk (s^2 + s_{1n}^2)(s^2 + s_{2n}^2)} \left[ \frac{\cos(\psi)s - \sin(\psi)\alpha_n}{s^2 + \alpha_n^2} + \frac{-\cos(\psi)s + \sin(\psi)\beta_n}{s^2 + \beta_n^2} \right] \quad (52)$$

Finally, by taking the inverse Laplace transform, the following solutions are obtained:

$$\begin{aligned} p_n(\tau) &= \tilde{p}_{1n} \cos(s_{1n} \tau) + \tilde{p}_{2n} \sin(s_{1n} \tau) + \tilde{p}_{3n} \cos(s_{2n} \tau) + \tilde{p}_{4n} \sin(s_{2n} \tau) + \tilde{p}_{5n} \cos(\alpha_n \tau) + \tilde{p}_{6n} \sin(\alpha_n \tau) \\ &\quad + \tilde{p}_{7n} \cos(\beta_n \tau) + \tilde{p}_{8n} \sin(\beta_n \tau) \end{aligned} \quad (53)$$

$$q_n(\tau) = \tilde{q}_{1n} \cos(s_{1n}\tau) + \tilde{q}_{2n} \cos(s_{1n}\tau) + \tilde{q}_{3n} \cos(s_{2n}\tau) + \tilde{q}_{4n} \cos(s_{2n}\tau) + \tilde{q}_{5n} \cos(\alpha_n\tau) + \tilde{q}_{6n} \sin(\alpha_n\tau) + \tilde{q}_{7n} \cos(\beta_n\tau) + \tilde{q}_{8n} \sin(\beta_n\tau) \tag{54}$$

where  $\tilde{p}_i$  and  $\tilde{q}_i$ , for  $i = 1, 2, \dots, 8$ , are given in Appendix A.

Similar to the Euler-Bernoulli Nano beam, the existence of critical velocities should be investigated. The following four cases should be examined:

$$s_{1n} = \alpha_n, s_{1n} = \beta_n, s_{2n} = \alpha_n \quad \text{and} \quad s_{2n} = \beta_n \tag{55}$$

For the sake of brevity, we examine the first case only:

$$s_{1n} = \alpha_n \Rightarrow v_{ncr\alpha}^T = \frac{L}{n\pi} (\Omega - \Omega_{1n}^T) \tag{56}$$

where the superscript  $T$  stands for the Timoshenko beam model;  $\Omega_{1n}^T$  is defined below:

$$\Omega_{1n}^T = \frac{s_{1n}}{T} = \frac{1}{T\sqrt{2(1+\mu^2\gamma_n^2)}} \sqrt{\left( \frac{(1+\lambda^2\gamma_n^2)(\bar{k} + \bar{A}\gamma_n^2) - \gamma_n^2(1+\lambda^2\gamma_n^2) + \bar{H}\gamma_n^2(1+\mu^2\gamma_n^2)}{\bar{k}} \right)^2 + \frac{4\bar{k}\gamma_n^2(1+\lambda^2\gamma_n^2)(1+\lambda^2\gamma_n^2)}{\bar{k}}} \sqrt{(1+\lambda^2\gamma_n^2)(\bar{k} + \bar{A}\gamma_n^2) + \frac{\gamma_n^2(1+\lambda^2\gamma_n^2) + \bar{H}\gamma_n^2(1+\mu^2\gamma_n^2)}{\bar{k}}} \tag{57}$$

Corresponding to this case, for capturing the dynamic response, Eqs. (51) and (52) should be reconstructed as follows:

$$\bar{Q}_n = \frac{-f_0 d_{1n}}{kAG\bar{k}(s^2 + \alpha_n^2)(s^2 + s_{2n}^2)} \left[ \frac{\cos(\psi)s - \sin(\psi)\alpha_n}{s^2 + \alpha_n^2} + \frac{-\cos(\psi)s + \sin(\psi)\beta_n}{s^2 + \beta_n^2} \right] \tag{58}$$

$$\bar{P}_n = \frac{f_0 (s^2 + c_{1n})}{kAG\bar{k}(s^2 + \alpha_n^2)(s^2 + s_{2n}^2)} \left[ \frac{\cos(\psi)s - \sin(\psi)\alpha_n}{s^2 + \alpha_n^2} + \frac{-\cos(\psi)s + \sin(\psi)\beta_n}{s^2 + \beta_n^2} \right] \tag{59}$$

The inverse Laplace transform of the above relations is given in Appendix A. The other remaining cases can be examined by the same manner. It has to be noted that- the governing equations of the modified nonlocal strain gradient Timoshenko Nano beam (i.e. Eqs. (29) -(30), proposed in this study) are solved exactly by the same method which, for the sake of brevity, will not be presented here.

#### 4 RESULTS AND DISCUSSIONS

So far, the size-dependent vibrations of Euler-Bernoulli and Timoshenko Nano beam s with surface effects acted upon by moving harmonic loads in the frameworks of nonlocal strain gradient elasticity theory have been carried out theoretically. In this regard, by using the Galerkin discretization method in conjunction with the Laplace transform method, some analytical solutions for the cases of simply supported boundary conditions have been derived. Extension of the presented method of solution towards the other boundary conditions is straightforward.

In this section, the numerical results will be presented. Before doing that, it is necessary to validate the derived formulas in the previous section. In this regard, in the following, we will compare our results with those already presented in the literature.

#### 4.1 Comparison studies

In the first attempt, a comparison study is established to evaluate the accuracy and performance of the derived solution of the Euler-Bernoulli beam model. In a paper by Şimşek [15], the size-dependent forced vibration of a simply supported SWCNT acted upon by a concentrated moving load, by using the nonlocal Euler-Bernoulli beam theory, has been examined. In Table 1., the computed maximum non-dimensional dynamic deflections of a simply supported SWCNT are compared with those reported in Ref [15]. To this end, we have normalized the dynamic deflection by the static deflection of the SWCNT under a point load at its midpoint, i.e.  $w_s = f_0 L^3 / 48EI$ . To investigate the effects of the velocity and excitation frequency of the moving harmonic load on the dynamic responses of the Nano beam s, the following dimensionless velocity and frequency parameters namely  $\alpha$  and  $\beta$ , respectively, are defined as:

$$\alpha = \frac{\pi v}{L \omega_1}, \beta = \frac{\Omega}{\omega_1} \quad (60)$$

where  $\omega_1$  is the fundamental natural frequency of the SWCNT. It is worth to mention that in this comparison study we have set  $l = H = E_s = 0$ ., also it has been assumed that the amplitude of the moving harmonic load is varied with time by a pure sine function. This can be achieved by setting  $\psi = 0$  in Eq. (31) and the subsequent relations. Computations are carried out by taking the following values as considered in Ref. [15]:

$E = 1TPa, \rho = 2300 kg / m^3, d = 1nm$  and  $h = 0.34 nm$ . As seen from Table 1., close agreement between our results and those of Ref. [15] is observed. This ensures us about the accuracy and effectiveness of our computer codes related to the Euler-Bernoulli beam Nano beam s. Also, it is seen from Table., that the contribution of higher-order modes can be neglected because the first mode is the most significant. Hence in subsequent numerical results, the first three natural modes are chosen.

**Table 1**

Convergence study of the dynamic deflections of the SWCNT (simply supported Euler-Bernoulli beam model) and their comparison with those of Ref [15].

ea (nm)	Number of modes	Maximum non-dimensional dynamic deflection for $L/d=10$						
		$\alpha = 0.1, \beta = 1$		$\alpha = 0.5, \beta = 1$		$\alpha = 1, \beta = 1$		
		Ref. [15]	Present study	Ref. [15]	Present study	Ref. [15]	Present study	
0	1	9.63587	9.63856	1.08150	1.08152	1.31403	1.31405	
	2	9.63587	9.63856	1.08150	1.08152	1.32248	1.32249	
	3	9.63592	9.63879	1.07858	1.07860	1.32471	1.32473	
	4	9.63592	9.63879	1.07858	1.07860	1.32459	1.32461	
	6	9.63592	9.63878	1.07828	1.07830	1.32455	1.32457	
	8	9.63592	9.63878	1.07822	1.07823	1.32456	1.32457	
	10	9.63592	9.63878	1.07820	1.07821	1.32456	1.32457	
	12	9.63592	9.63878	1.07820	1.07821	1.32456	1.32457	
	14	9.63592	9.63878	1.07819	1.07821	1.32456	1.32457	
	2	1	13.43997	13.44370	1.50846	1.50849	1.83279	1.83281
		2	13.43997	13.44370	1.52643	1.52646	1.85618	1.83281
		3	13.44184	13.44630	1.52081	1.52083	1.92403	1.92268
		4	13.44184	13.44630	1.52068	1.52071	1.92405	1.92268
		6	13.44205	13.44610	1.51849	1.51852	1.91513	1.91582
8		13.44194	13.44610	1.51780	1.51782	1.91741	1.91582	
10		13.44195	13.44610	1.51769	1.51772	1.91662	1.91482	
12		13.44192	13.44610	1.51764	1.51767	1.91692	1.91482	
14		13.44193	13.44610	1.51781	1.51784	1.91678	1.91482	

In the second attempt, regarding the Timoshenko beam model, the derived solutions, i.e. Eqs. (53) -(54), have to be validated. To do this, Eqs. (53)-(54) have been reduced to the conventional nonlocal Timoshenko beam model subjected to a concentrated moving force by setting  $\Omega = 0, \psi = \pi / 2$  and  $l = 0$ . Kiani and Mehri [7] have presented

some analytical solutions for nonlocal Timoshenko Nano beam s subjected to a concentrated moving force. In Fig.2, we have compared the normalized dynamic deflection of our reduced model with that of Ref. [7]. In this comparison, the normalized dimensionless deflection  $W_N$  and the normalized velocity parameter  $V_N = v / v_{cr}^E$  have been used. Also, the slenderness ratio of the Nano beam has been set to  $ar = L / d = 10$ . The other geometrical and physical properties of the Nano beam have been adopted from Ref. [7]. As seen from this figure, our reduced analytical solution matches exactly with that of Kiani and Mehri [7].

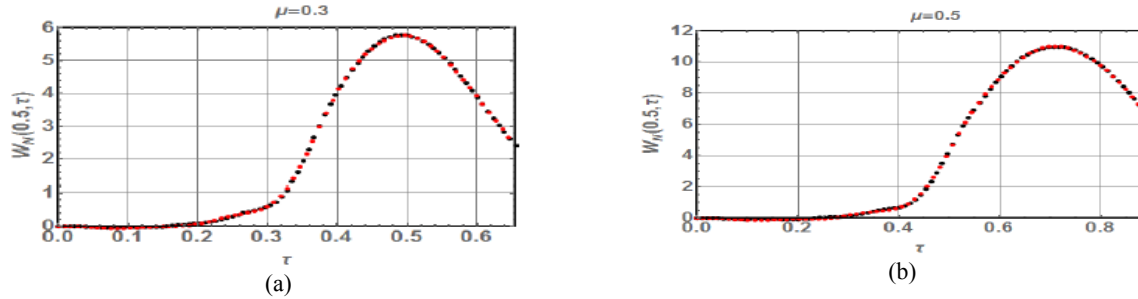


**Fig.2**

Time histories of the normalized dynamic deflections at the midspan of the reduced Timoshenko Nano beam for  $ar = 10, V_N = 0.7$ .

## 4.2 Numerical results

Now, we continue this subsection by presenting some numerical results. In this subsection, the following bulk properties, corresponding to a SWCNT, are adopted from Ref. [15]:  $E = 1TPa$  and  $\rho = 2300kg / m^3$ . Also, the effective wall thickness of  $0.34 nm$  is adopted. For investigating the effect of the material length scale parameter, the nonlocal parameter, the surface elastic modulus and the residual surface tension on the dynamics response, we will vary one at a time. In other words, to investigate the effect of one specific parameter on the dynamic response, we vary it in an adopted range while the other parameters are held constant.

### 4.2.1 Effect of the nonlocal and material length scale parameters

It is well-known that the nonlocal parameter is commonly taken into account in the range of [0-2] nm for the vibration analysis of carbon nanotubes in the literature. Hence in this study, we obey that rule and vary the nonlocal parameter  $ea$ , in that range. For the material length scale parameter such a common range has not been reported in the literature yet. By the way, for investigating the effect of both of the length scales, concurrently, on the dynamic response of Nano beam s (in this case SWCNTs), we introduce a dimensionless length scale factor as  $SF = l / ea = \lambda / \mu$ . In this subsection, for numerical calculations, consider a SWCNT with the surface elastic modulus  $E_s = 35.3N / m$  and the residual surface tension  $\tau_0 = 0.31N / m$ , adopted from Ref. [59]. The parameters of the moving harmonic load are taken as  $v = 5nm / ns, \psi = 0$  and  $\Omega = a_\omega \omega_1^E$ ; where  $a_\omega$  is a constant and  $\omega_1^E$  is the fundamental natural circular frequency of a Nano beam predicted by classical Euler-Bernoulli beam model without surface effects. The mean diameter of the SWCNT is  $1 nm$ . Fig.3 shows variation of the maximum normalized dimensionless dynamic deflection of a moderately short and thick SWCNT, predicted by the nonlocal strain gradient Euler-Bernoulli (*E-B*), Timoshenko (*T*) and modified Timoshenko (*MT*) beam models, with the scale parameter for various values of the excitation frequency. As can be seen from this figure, when  $SF=1$ , the dynamic responses are identical. It can be shown that when the material length scale parameter is equal to the nonlocal parameter, the nonlocal strain gradient dynamic response is identical with the classical one. For example, corresponding to the Euler-Bernoulli beam model, from Eqs. (34)-(35), it is evident that by setting  $\lambda = \mu$ , the classical response will be obtained. When  $SF < 1$  (or  $l < ea$ ), increasing the normalized nonlocal parameter leads to an increase in the dynamic deflection of the SWCNT at a certain value of the scale factor. However, when  $SF > 1$  (or  $l > ea$ ), the maximum normalized dimensionless dynamic deflection of the SWCNT will decrease with increasing the normalized nonlocal

parameter. These phenomena show that the nonlocal strain gradient theory predicts a stiffness-softening effect when  $ea > l$  (like the nonlocal elasticity theory), and predicts a stiffness-hardening effect when  $ea < l$  (like the strain gradient theory). As expected, the Euler-Bernoulli beam model differs considerably from the Timoshenko beam model. This is attributed to the fact that the Nano beam is relatively short and thick.

As mentioned previously, the exclusion of nonlocality in the shear constitutive relation leads to a modification to the nonlocal Timoshenko beam model. It has been shown that the modified Timoshenko beam model predicts almost the same natural frequencies compared with the original one. Based on this modification, in a similar way, Naderi and Saidi [60] have proposed the same modification in the nonlocal Mindlin plate theory and shown that the critical buckling loads predicted by the modified nonlocal Mindlin plate theory differ significantly from those predicted by the nonlocal Mindlin plate theory. In this study, we have exerted that modification to the nonlocal strain gradient Timoshenko beam model for the first time. As can be seen from Fig.3, the dynamic deflections predicted by the modified nonlocal strain gradient Timoshenko beam model differ from those predicted by the nonlocal strain gradient Timoshenko beam model. The difference is more significant in the initial part and terminal part of the figure. In other words, when  $SF < 1$ , the modification exerts a stiffness-hardening effect, it and exerts a stiffness-softening effect when  $SF > 1$ . As the last observation, it has to be mentioned that for higher values of the nonlocal parameter, the aforementioned difference between the two theories are more significant.

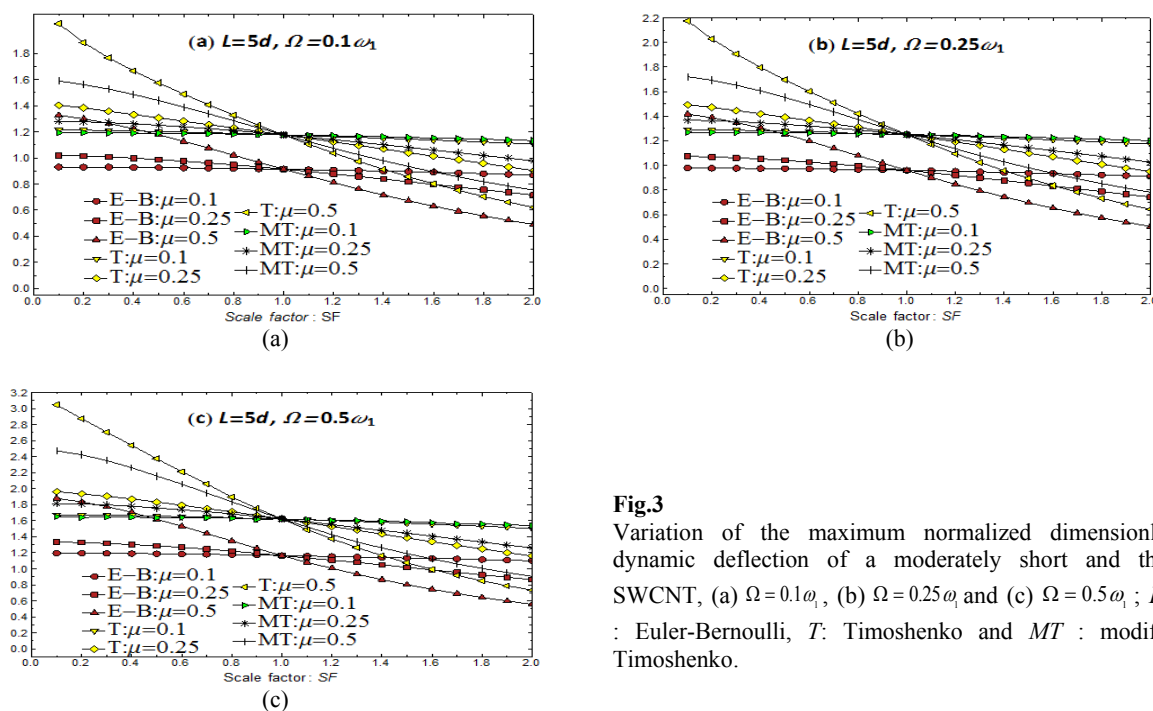


**Fig.3**

Variation of the maximum normalized dimensionless dynamic deflection of a moderately short and thick SWCNT, (a)  $\Omega = 0.1\omega_1$ , (b)  $\Omega = 0.25\omega_1$  and (c)  $\Omega = 0.5\omega_1$ ; E-B : Euler-Bernoulli, T: Timoshenko and MT : modified Timoshenko.

#### 4.2.2 Effects of velocity, excitation frequency and phase angle of the moving harmonic load

In this subsection, the effect of the velocity, excitation frequency and the phase angle of the moving harmonic load on the dynamic response of SWCNTs has to be examined. In the first attempt, we examine the significance of the velocity of the moving harmonic load in our analysis.

For the physical and geometrical properties given in the previous subsection, Fig.4 shows variation of the maximum normalized dimensionless dynamic deflection of the SWCNT with the velocity parameter. As seen from this figure, increasing the velocity parameter will gradually decrease the maximum normalized dimensionless dynamic deflection. Also, it can be observed that for lower values of the velocity parameter, the modified nonlocal strain gradient Timoshenko beam model differs more significantly from the nonlocal strain gradient Timoshenko beam model. Another important observation is the existence of the global maxima and local minima. In other words, by increasing the velocity of the moving harmonic load, the maximum normalized dimensionless dynamic deflection, after experiencing some local fluctuations, increases to a global maximum. Further increase in the value

of the velocity of the moving harmonic load will decrease the maximum normalized dimensionless dynamic deflection.

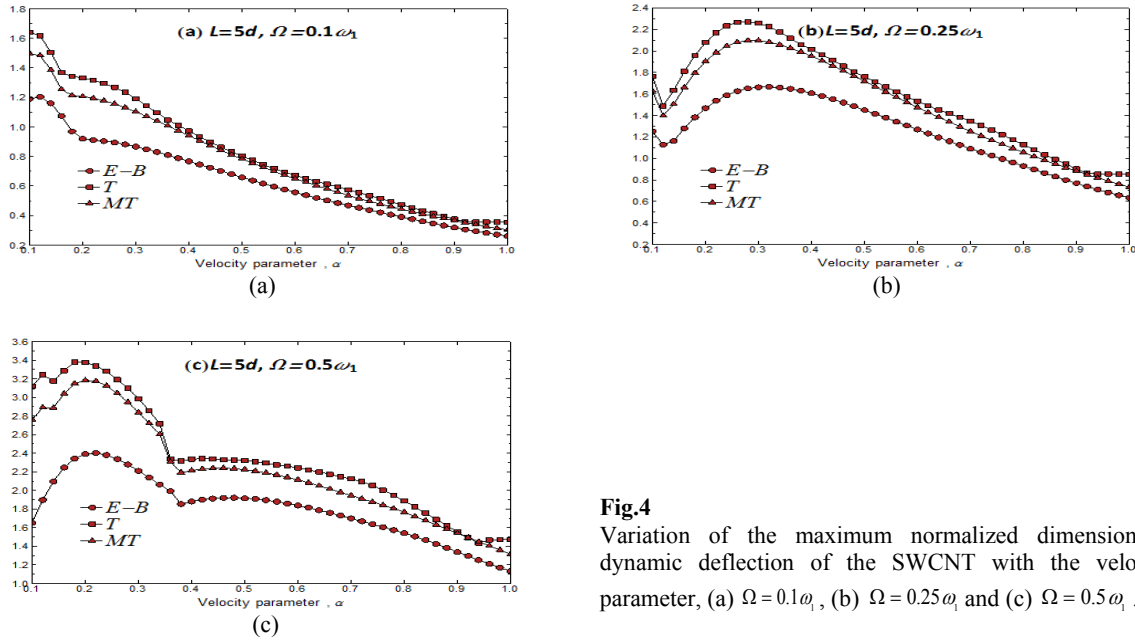


**Fig.4** Variation of the maximum normalized dimensionless dynamic deflection of the SWCNT with the velocity parameter, (a)  $\Omega = 0.1\omega_1$ , (b)  $\Omega = 0.25\omega_1$  and (c)  $\Omega = 0.5\omega_1$ .

The other important parameter related to the moving harmonic load is the excitation frequency  $\Omega$ . In Fig.5, the computed values of the maximum normalized dimensionless dynamic deflection of the SWCNT have been shown. As can be seen from this figure, increasing the frequency parameter towards a certain value leads to an increase in the value of the dynamic deflection. Further increase in the frequency parameter decreases the dynamic deflection. That certain value of the frequency parameter is over predicted by the Euler-Bernoulli beam model compared to the Timoshenko/modifies Timoshenko beam model. An important fact that one should pay attention to it is that in this study we have restricted ourselves to the linear vibration analysis, accordingly, the presented plots in Fig.5 around the peak values are not truly correct. Around these regions, the nonlinear analysis should be employed.

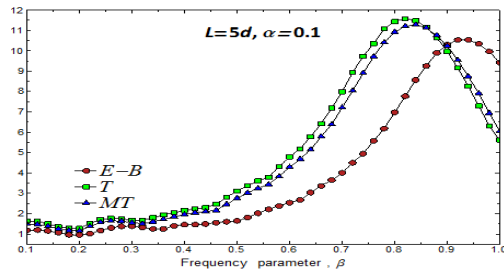


**Fig.5** Variation of the maximum normalized dimensionless dynamic deflection of the SWCNT with the velocity parameter.

By another numerical example, in Fig.6, the variation of the lowest critical velocity parameter, which is the ratio of the lowest critical velocity to  $L\omega_1/\pi$ , is presented. As seen from this figure, some observations can be deduced as follows:

- First, threshold values of the frequency parameter are observed. One can expect this phenomenon from the closed-form relations, regarding to the critical velocities, presented in the previous section. By this statement, we mean that there exist certain values of  $\beta$ , which for those values of  $\beta$  below/over these thresholds an increase in the frequency parameter leads to the a/an decrease/increase in the value of the lowest critical parameter.
- Second, from panel (a) it can be observed that for a certain value of the frequency parameter, below the related threshold value, increasing the material characteristic parameter (in this case it is equivalent to increasing the scale factor too), increases the lowest critical velocity. However, for those values of the frequency parameter higher than the threshold values, up to certain values of the frequency parameter, the

same behavior is observed. By passing these certain values further increase in the frequency parameter will decrease the lowest critical velocity.

- Third, from panel (b), one can draw same conclusions as stated for panel (a). But the difference is that the material characteristic parameter and the nonlocal parameter have reverse effects on the lowest critical velocity parameter.
- Fourth, for those values of the frequency parameter below the thresholds, the Euler-Bernoulli beam model predicts higher values of the lowest critical velocity than the two Timoshenko beam models and for those values of the frequency parameter over the thresholds, it predicts lower values of the lowest critical velocity than the two Timoshenko beam models.

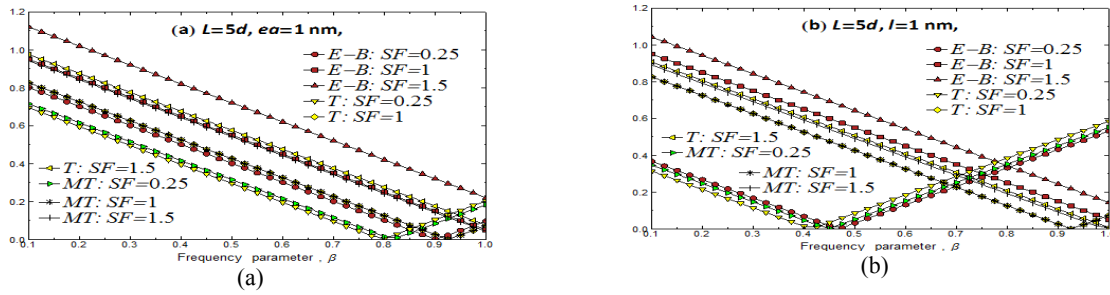


**Fig.6**

Variation of the lowest critical velocity with the frequency parameter, (a)  $ea=1 \text{ nm}$  and (b)  $l=1 \text{ nm}$ .

#### 4.2.3 Effect of the surface elasticity parameters

In this subsection, the effect of the surface modulus and the residual surface tension on the dynamic response of a Nano beam has been examined. In the numerical calculations, we again consider the SWCNT used in previous examples with the following parameters:  $ea = 1.0 \text{ nm}$ ,  $l = 0.5 \text{ nm}$ ,  $L = 5d$  and  $\alpha = 0.1$ . It has to be noted that the value of the surface modulus depends on the material type and the surface crystal orientation [52]. For example by using (1 1 2) nickel, using the atomistic calculations, the related value of  $E_s = 35.3 \text{ N/m}$  has been obtained [61]. In this study, for the purpose of theoretical investigation, we have varied the surface elastic modulus in a positive range.

In Fig.7, the variation of the maximum normalized dynamic deflection with the surface elastic modulus has been shown. As seen from this figure, increasing the surface elastic modulus decreases the maximum dynamic deflection for the three beam models. The modified nonlocal strain gradient Timoshenko beam model, proposed in this study, predicts lower values for the maximum normalized dimensionless dynamic deflection compared to the nonlocal strain gradient Timoshenko beam model. Also, among the three beam models, the Euler-Bernoulli beam model predicts the lowest values of the dynamic deflection. By comparing panel (b) with panel (a), it can be concluded that an increase in the slenderness ratio of the SWCNT leads to a decrease in the value of the normalized dynamic deflection. From panel (b), it can be seen that, corresponding to a longer SWCNT, the results predicted by the modified nonlocal strain gradient Timoshenko beam model differ slightly from those predicted by the nonlocal strain gradient Timoshenko beam model.

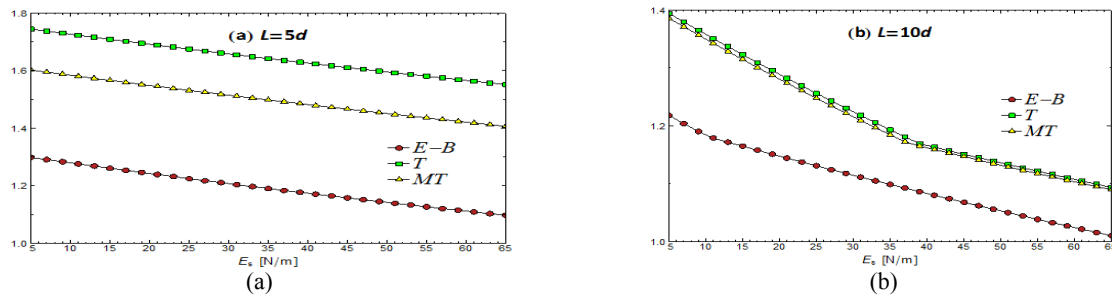


**Fig.7**

Variation of the maximum normalized dynamic deflection of the SWCNT with the surface elastic modulus, (a)  $L=5d$  and (b)  $L=10d$ .

## 5 CONCLUSIONS

In this study, we have carried out the forced vibration problem of Nano beam s acted upon by moving harmonic loads. To do this, we have derived the governing equations of forced vibration of three beam models namely, the Euler-Bernoulli, Timoshenko and modified Timoshenko beam models in the frameworks of the nonlocal strain gradient elasticity theory. Based on a combination of the Galerkin and Laplace transform methods, analytical solutions have been obtained for simply supported boundary conditions. However, the extension to other boundary conditions is straightforward. As explained in the text, a modification has been introduced to the nonlocal strain gradient Timoshenko beam model for the first time. The modification has been exerted to the constitutive equations by exclusion of the nonlocality in the shear constitutive relation. The most important findings are summarized below:

- When  $SF=1$  (it means that the material characteristic parameter is equal to the nonlocal parameter), the dynamic responses predicted by the three beam models are identical with the results by the associated classical beam models. In other words, for this case, the presence of material characteristic parameter in the formulations cancel the effect of the nonlocal parameter out.
- When the material characteristic parameter is smaller than the nonlocal parameter (i.e.,  $SF<1$ ), increasing the nonlocal parameter leads to an increase in the dynamic deflection of Nano beam s at a certain value of the scale factor (it corresponds to stiffness-softening phenomenon). When the material characteristic parameter is higher than the nonlocal parameter (i.e.,  $SF>1$ ), the dynamic deflection of Nano beam s will decrease with increasing the nonlocal parameter (it corresponds to stiffness-hardening phenomenon). Based on these observations, it can be concluded that the nonlocal parameter and the material characteristic parameter have completely reverse effects on the dynamic response of Nano beam s.
- The modified nonlocal strain gradient Timoshenko beam model differs considerably from the nonlocal strain gradient Timoshenko beam model. The difference is more relevant for lower values of the slenderness ratio. When  $SF<1$ , the modified model predicts lower values for the dynamic deflection compared to those predicted by the unmodified model. When  $SF>1$ , the modified model predicts higher values for the dynamic deflection compared to those predicted by the non-modified model.
- Increasing the velocity of the moving harmonic load up to a certain value will increase the dynamic deflection of Nano beam s. Further increase in the velocity of the moving harmonic load decreases the dynamic deflection.
- Increasing the excitation frequency of the moving harmonic load up to a certain value increases the dynamic deflection. Further increase in the excitation frequency leads to a decrease in the values of the dynamic deflection.
- Closed-form relations have been obtained for the critical velocities. We have examined the lowest critical velocity and shown that it varies linearly with the excitation frequency. Increasing the excitation frequency up to a certain value will decrease the lowest critical velocity. By passing this point, further increase in the excitation frequency increases the lowest critical velocity.
- Increasing the surface elastic modulus will decrease the dynamic deflection.

## APPENDIX A

The constants appearing in Eq. (40) are summarized below:

$$c_{an} = \frac{f_1}{\omega_n^2 - \alpha_n^2}, s_{an} = \frac{f_2}{\alpha_n^2 - \omega_n^2}, c_{\beta n} = \frac{f_1}{\beta_n^2 - \omega_n^2}, s_{\beta n} = \frac{f_2}{\omega_n^2 - \beta_n^2}, c_{\omega n} = \frac{f_1(\beta_n^2 - \alpha_n^2)}{(\omega_n^2 - \beta_n^2)(\omega_n^2 - \alpha_n^2)}, s_{\omega n} = \frac{f_2(\alpha_n \beta_n + \omega_n^2)(\alpha_n - \beta_n)}{\omega_n(\omega_n^2 - \beta_n^2)(\omega_n^2 - \alpha_n^2)} \quad (\text{A.1})$$

The constants appearing in Eq. (44) are summarized below:

$$a_{ncr\beta} = \frac{-f_1}{\alpha_n^2 - \omega_n^2}, b_{ncr\beta} = \frac{f_2}{\alpha_n^2 - \omega_n^2}, c_{ncr\beta} = \frac{f_1}{\alpha_n^2 - \omega_n^2}, d_{ncr\beta} = \frac{-f_2}{2\omega_n}, e_{ncr\beta} = \frac{f_2}{2\omega_n^2} - \frac{\alpha_n f_2}{\omega_n(\alpha_n^2 - \omega_n^2)}, f_{ncr\beta} = -\frac{f_1}{2\omega_n} \quad (\text{A.2})$$

$$a_{ncr\alpha} = \frac{f_1}{\beta_n^2 - \omega_n^2}, b_{ncr\alpha} = \frac{-f_2}{\beta_n^2 - \omega_n^2}, c_{ncr\alpha} = \frac{-f_1}{\beta_n^2 - \omega_n^2}, d_{ncr\alpha} = \frac{f_2}{2\omega_n}, e_{ncr\alpha} = \frac{-f_2}{2\omega_n^2} + \frac{\beta_n f_2}{\omega_n(\beta_n^2 - \omega_n^2)}, f_{ncr\alpha} = \frac{f_1}{2\omega_n}$$

The constants appearing in Eqs. (53) and (54) are summarized below:

$$\begin{aligned}
\tilde{p}_{1n} &= \frac{\cos(\psi)(\alpha_n^2 - \beta_n^2)}{\Sigma_{1n}}, \tilde{p}_{2n} = \frac{\sin(\psi)(\alpha_n \beta_n + s_{1n}^2)(\beta_n - \alpha_n)}{s_{1n} \Sigma_{1n}}, \tilde{p}_{3n} = \frac{\cos(\psi)(\beta_n^2 - \alpha_n^2)}{\Sigma_{2n}}, \tilde{p}_{4n} = \frac{\sin(\psi)(\alpha_n \beta_n + s_{2n}^2)(\alpha_n - \beta_n)}{s_{2n} \Sigma_{2n}}, \\
\tilde{p}_{5n} &= \frac{c_{1n} f_0 \cos(\psi)}{kAGk \overline{(\alpha_n^2 - s_{1n}^2)(s_{2n}^2 - \alpha_n^2)}}, \tilde{p}_{6n} = \frac{-c_{1n} f_0 \sin(\psi)}{kAGk \overline{(s_{1n}^2 - \alpha_n^2)(s_{2n}^2 - \alpha_n^2)}}, \tilde{p}_{7n} = \frac{-c_{1n} f_0 \cos(\psi)}{kAGk \overline{(s_{1n}^2 - \beta_n^2)(s_{2n}^2 - \beta_n^2)}}, \\
\tilde{p}_{8n} &= \frac{c_{1n} f_0 \sin(\psi)}{kAGk \overline{(s_{1n}^2 - \beta_n^2)(s_{2n}^2 - \beta_n^2)}}, \tilde{q}_{1n} = \frac{\cos(\psi)(d_{1n} - s_{1n}^2)(\alpha_n^2 - \beta_n^2)}{\Sigma_{3n}}, \tilde{p}_{2n} = \frac{\sin(\psi)(\alpha_n - \beta_n)(\alpha_n \beta_n + s_{1n}^2)(s_{1n}^2 - d_{1n})}{s_{1n} \Sigma_{3n}}, \\
\tilde{p}_{3n} &= \frac{(\alpha_n^2 - \beta_n^2)(s_{2n}^2 - d_{1n}) \cos(\psi)}{\Sigma_{4n}}, \tilde{p}_{4n} = \frac{\sin(\psi)(d_{1n} - s_{2n}^2)(\alpha_n \beta_n + s_{2n}^2)(\alpha_n - \beta_n)}{s_{2n} \Sigma_{4n}}, \tilde{p}_{5n} = \frac{-f_0 \cos(\psi)(d_{1n} - \alpha_n^2)}{kAGk \overline{(s_{1n}^2 - \alpha_n^2)(s_{2n}^2 - \alpha_n^2)}}, \\
\tilde{p}_{6n} &= \frac{f_0 (d_{1n} - \alpha_n^2) \sin(\psi)}{kAGk \overline{(s_{1n}^2 - \alpha_n^2)(s_{2n}^2 - \alpha_n^2)}}, \tilde{p}_{7n} = \frac{f_0 (d_{1n} - \beta_n^2) \cos(\psi)}{kAGk \overline{(s_{1n}^2 - \beta_n^2)(s_{2n}^2 - \beta_n^2)}}, \tilde{p}_{8n} = \frac{-f_0 (d_{1n} - \beta_n^2) \sin(\psi)}{kAGk \overline{(s_{1n}^2 - \beta_n^2)(s_{2n}^2 - \beta_n^2)}},
\end{aligned} \tag{A.3}$$

where

$$\begin{aligned}
s_{1n} &= \sqrt{\frac{d_{1n} + c_{2n} + \sqrt{(d_{1n} - c_{2n})^2 + 4c_{1n}d_{2n}}}{2}}, s_{2n} = \sqrt{\frac{d_{1n} + c_{2n} - \sqrt{(d_{1n} - c_{2n})^2 + 4c_{1n}d_{2n}}}{2}}, \\
\Sigma_{1n} &= \frac{kAGk \overline{(s_{1n}^2 - s_{2n}^2)(s_{1n}^2 - \alpha_n^2)(s_{1n}^2 - \beta_n^2)}}{c_{1n} f_0}, \Sigma_{2n} = \frac{kAGk \overline{(s_{1n}^2 - s_{2n}^2)(s_{2n}^2 - \alpha_n^2)(s_{2n}^2 - \beta_n^2)}}{c_{1n} f_0}, \\
\Sigma_{3n} &= \frac{kAGk \overline{(s_{1n}^2 - s_{2n}^2)(s_{1n}^2 - \alpha_n^2)(s_{1n}^2 - \beta_n^2)}}{f_0}, \Sigma_{4n} = \frac{kAGk \overline{(s_{1n}^2 - s_{2n}^2)(s_{2n}^2 - \alpha_n^2)(s_{2n}^2 - \beta_n^2)}}{f_0}
\end{aligned} \tag{A.4}$$

The inverse Laplace transform of Eqs. (58) and (59) are given in the following:

$$\begin{aligned}
p_n(\tau) &= \hat{p}_{1n} \cos(s_{2n} \tau) + \hat{p}_{2n} \sin(s_{2n} \tau) + \hat{p}_{3n} \cos(\alpha_n \tau) + \hat{p}_{4n} \sin(\alpha_n \tau) \\
&\quad + \hat{p}_{5n} \cos(\beta_n \tau) + \hat{p}_{6n} \sin(\beta_n \tau) \text{ for the case of } \nu = \nu_{ncr\alpha}^T
\end{aligned} \tag{A.5}$$

$$\begin{aligned}
q_n(\tau) &= \hat{q}_{1n} \cos(s_{2n} \tau) + \hat{q}_{2n} \cos(s_{2n} \tau) + \hat{q}_{3n} \cos(\alpha_n \tau) + \hat{q}_{4n} \sin(\alpha_n \tau) \\
&\quad + \hat{q}_{5n} \cos(\beta_n \tau) + \hat{q}_{6n} \sin(\beta_n \tau) \text{ for the case of } \nu = \nu_{ncr\alpha}^T
\end{aligned} \tag{A.6}$$

where

$$\begin{aligned}
\hat{p}_{1n} &= \frac{c_{1n} f_0 (\alpha_n^2 - \beta_n^2) \cos(\psi)}{kAGk \overline{(\alpha_n^2 - s_{2n}^2)^2 (s_{2n}^2 - \beta_n^2)}}, \hat{p}_{2n} = \frac{-c_{1n} f_0 (\alpha_n - \beta_n)(\alpha_n \beta_n + s_{2n}^2) \sin(\psi)}{kAGk \overline{(\alpha_n^2 - s_{2n}^2)^2 (s_{2n}^2 - \beta_n^2)} s_{2n}}, \\
\hat{p}_{3n} &= \frac{c_{1n} f_0 \left( \cos(\psi)(2s_{2n}^2 \alpha_n - 4\alpha_n^3 + 2\alpha_n \beta_n^2) + \sin(\psi)(s_{2n}^2 \alpha_n^2 - \alpha_n^4 - s_{2n}^2 \beta_n^2 + \alpha_n^2 \beta_n^2) \tau \right)}{2kAGk \overline{(\alpha_n^2 - s_{2n}^2)^2 (\beta_n^2 - \alpha_n^2)} \alpha_n}, \\
\hat{p}_{4n} &= \frac{-c_{1n} f_0 \left( \cos(\psi)(-s_{2n}^2 \alpha_n^3 + \alpha_n^5 + s_{2n}^2 \alpha_n \beta_n^2 - \alpha_n^3 \beta_n^2) \tau + \sin(\psi)(s_{2n}^2 \alpha_n^2 - 3\alpha_n^4 + 2s_{2n}^2 \alpha_n \beta_n - 2\alpha_n^3 \beta_n - s_{2n}^2 \beta_n + 3\alpha_n^2 \beta_n^2) \right)}{2kAGk \overline{(\alpha_n^2 - s_{2n}^2)^2 (\alpha_n^2 - \beta_n^2)}}, \\
\hat{p}_{5n} &= \frac{c_{1n} f_0 \cos(\psi)}{kAGk \overline{(\beta_n^2 - s_{2n}^2)(\alpha_n^2 - \beta_n^2)}}, \hat{p}_{6n} = \frac{-c_{1n} f_0 \sin(\psi)}{kAGk \overline{(\beta_n^2 - s_{2n}^2)(\alpha_n^2 - \beta_n^2)}}, \\
\hat{q}_{1n} &= \frac{f_0 (d_{1n} - s_{2n}^2)(\alpha_n^2 - \beta_n^2) \cos(\psi)}{kAGk \overline{(\alpha_n^2 - s_{2n}^2)^2 (s_{2n}^2 - \beta_n^2)}}, \hat{q}_{2n} = \frac{-f_0 (d_{1n} - s_{2n}^2)(\alpha_n - \beta_n)(\alpha_n \beta_n + s_{2n}^2) \sin(\psi)}{kAGk \overline{(\alpha_n^2 - s_{2n}^2)^2 (s_{2n}^2 - \beta_n^2)}}, \\
\hat{q}_{3n} &= \frac{f_0 \cos(\psi) \left( d_{1n} (s_{2n}^2 - 2\alpha_n^2 + \beta_n^2) - \alpha_n^4 - s_{2n}^2 \beta_n^2 \right)}{kAGk \overline{(\alpha_n^2 - s_{2n}^2)^2 (\alpha_n^2 - \beta_n^2)}} + \frac{f_0 (\alpha_n^2 - d_{1n}) \tau}{2kAGk \overline{(\alpha_n^2 - s_{2n}^2) \alpha_n}}
\end{aligned} \tag{A.7}$$

$$\hat{q}_{4n} = \frac{f_0 \cos(\psi)(\alpha_n^2 - d_{1n})\tau}{2kAG\bar{k}(\alpha_n^2 - s_{2n}^2)} + \frac{f_0 \sin(\psi) \left( s_{2n}^2 (\alpha_n^4 - 2\alpha_n^3 \beta_n - \alpha_n^2 \beta_n^2) + \alpha_n^6 + 2\alpha_n^5 \beta_n - \alpha_n^4 \beta_n^2 + d_{1n} (-3\alpha_n^4 - 2\alpha_n^3 \beta_n + 3\alpha_n^2 \beta_n^2 + s_{2n}^2 (\alpha_n^2 + 2\alpha_n \beta_n - \beta_n^2)) \right) \tau}{2kAG\bar{k}(\alpha_n^2 - s_{2n}^2)^2 (\beta_n^2 - \alpha_n^2)}, \quad (\text{A.7})$$

$$\hat{q}_{5n} = \frac{f_0 (d_{1n} - \beta_n^2) \cos(\psi)}{kAG\bar{k}(\beta_n^2 - s_{2n}^2)(\alpha_n^2 - \beta_n^2)}, \quad \hat{q}_{6n} = \frac{-f_0 (d_{1n} - \beta_n^2) \sin(\psi)}{kAG\bar{k}(\beta_n^2 - s_{2n}^2)(\alpha_n^2 - \beta_n^2)}$$

## ACKNOWLEDGMENTS

The figures for this article have been created using the SciDraw scientific figure preparation system [Caprio M. A., 2005, *Computer Physics Communications* **171**: 107].

## REFERENCES

- [1] Kiani K., 2010, Longitudinal and transverse vibration of a single-walled carbon nanotube subjected to a moving nanoparticle accounting for both nonlocal and inertial effects, *Physica E: Low-dimensional Systems and Nanostructures* **42**(9): 2391-2401.
- [2] Pijper D., 2005, Acceleration of a nanomotor: electronic control of the rotary speed of a light-driven molecular rotor, *Journal of the American Chemical Society* **127**(50): 17612-17613.
- [3] Shirai Y., 2005, Directional control in thermally driven single-molecule nanocars, *Nano Letters* **5**(11): 2330-2334.
- [4] Shirai Y., 2006, Surface-rolling molecules, *Journal of the American Chemical Society* **128**(14): 4854-4864.
- [5] Shirai Y., 2006, Recent progress on nanovehicles, *Chemical Society Reviews* **35**(11): 1043-1055.
- [6] Gross L., 2005, Trapping and moving metal atoms with a six-leg molecule, *Nature Materials* **4**(12): 892-895.
- [7] Kiani K., Mehri B., 2010, Assessment of nanotube structures under a moving nanoparticle using nonlocal beam theories, *Journal of Sound and Vibration* **329**(11): 2241-2264.
- [8] Kiani K., 2010, Application of nonlocal beam models to double-walled carbon nanotubes under a moving nanoparticle, Part I: Theoretical formulations, *Acta Mechanica* **216**(1-4): 165-195.
- [9] Kiani K., 2011, Nonlocal continuum-based modeling of a nanoplate subjected to a moving nanoparticle, Part I: Theoretical formulations, *Physica E: Low-dimensional Systems and Nanostructures* **44**(1): 229-248.
- [10] Kiani K., Wang Q., 2012, On the interaction of a single-walled carbon nanotube with a moving nanoparticle using nonlocal Rayleigh, Timoshenko, and higher-order beam theories, *European Journal of Mechanics - A/Solids* **31**(1): 179-202.
- [11] Kiani K., 2010, Application of nonlocal beam models to double-walled carbon nanotubes under a moving nanoparticle, Part II: Parametric study, *Acta Mechanica* **216**(1-4): 197-206.
- [12] Arani A.G., Roudbari M., Amir S., 2012, Nonlocal vibration of SWBNNT embedded in bundle of CNTs under a moving nanoparticle, *Physica B: Condensed Matter* **407**(17): 3646-3653.
- [13] Kiani K., 2011, Nonlocal continuum-based modeling of a nanoplate subjected to a moving nanoparticle, Part II: Parametric studies, *Physica E: Low-dimensional Systems and Nanostructures* **44**(1): 249-269.
- [14] Picu C., 2003, A nonlocal formulation of rubber elasticity, *International Journal for Multiscale Computational Engineering* **1**(1): 23-32.
- [15] Şimşek M., 2010, Vibration analysis of a single-walled carbon nanotube under action of a moving harmonic load based on nonlocal elasticity theory, *Physica E: Low-dimensional Systems and Nanostructures* **43**(1): 182-191.
- [16] Bazant Z.P., Jirásek M., 2002, Nonlocal integral formulations of plasticity and damage: survey of progress, *Journal of Engineering Mechanics* **128**(11): 1119-1149.
- [17] Jirasek M., 2004, Nonlocal theories in continuum mechanics, *Acta Polytechnica* **44**(5-6): 16-34.
- [18] Yi D., Wang T.C., Xiao Z., 2010, Strain gradient theory based on a new framework of non-local model, *Acta Mechanica* **212**(1-2): 51-67.
- [19] Akgöz B., Civalek Ö., 2011, Strain gradient elasticity and modified couple stress models for buckling analysis of axially loaded micro-scaled beams, *International Journal of Engineering Science* **49**(11): 1268-1280.
- [20] Akgöz B., Civalek Ö., 2012, Analysis of micro-sized beams for various boundary conditions based on the strain gradient elasticity theory, *Archive of Applied Mechanics* **82**(3): 423-443.
- [21] Wu J., Li X., Cao W., 2013, Flexural waves in multi-walled carbon nanotubes using gradient elasticity beam theory, *Computational Materials Science* **67**: 188-195.
- [22] Peddieson J., Buchanan G.R., McNitt R.P., 2003, Application of nonlocal continuum models to nanotechnology, *International Journal of Engineering Science* **41**(3): 305-312.
- [23] Lu P., 2006, Dynamic properties of flexural beams using a nonlocal elasticity model, *Journal of Applied Physics* **99**(7): 073510.
- [24] Reddy J., 2007, Nonlocal theories for bending, buckling and vibration of beams, *International Journal of Engineering Science* **45**(2): 288-307.

- [25] Murmu T., Pradhan S., 2009, Thermo-mechanical vibration of a single-walled carbon nanotube embedded in an elastic medium based on nonlocal elasticity theory, *Computational Materials Science* **46**(4): 854-859.
- [26] Askes H., Aifantis E.C., 2011, Gradient elasticity in statics and dynamics: an overview of formulations, length scale identification procedures, finite element implementations and new results, *International Journal of Solids and Structures* **48**(13): 1962-1990.
- [27] Tian Y., 2013, Ultrahard nanotwinned cubic boron nitride, *Nature* **493**(7432): 385-388.
- [28] Li X., 2010, Dislocation nucleation governed softening and maximum strength in nano-twinned metals, *Nature* **464**(7290): 877-880.
- [29] Lim C., Zhang G., Reddy J., 2015, A higher-order nonlocal elasticity and strain gradient theory and its applications in wave propagation, *Journal of the Mechanics and Physics of Solids* **78**: 298-313.
- [30] Ebrahimi F., Barati M.R., 2016, Flexural wave propagation analysis of embedded S-FGM Nano beam s under longitudinal magnetic field based on nonlocal strain gradient theory, *Arabian Journal for Science and Engineering* **2016**: 1-12.
- [31] Farajpour A., 2016, A higher-order nonlocal strain gradient plate model for buckling of orthotropic nanoplates in thermal environment, *Acta Mechanica* **2016**: 1-19.
- [32] Hosseini S., Rahmani O., 2016, Exact solution for axial and transverse dynamic response of functionally graded Nano beam under moving constant load based on nonlocal elasticity theory, *Meccanica* **2016**: 1-17.
- [33] Li L., Hu Y., 2016, Wave propagation in fluid-conveying viscoelastic carbon nanotubes based on nonlocal strain gradient theory, *Computational Materials Science* **112**: 282-288.
- [34] Li L., Hu Y., Li X., 2016, Longitudinal vibration of size-dependent rods via nonlocal strain gradient theory, *International Journal of Mechanical Sciences* **115**: 135-144.
- [35] Li L., 2016, Size-dependent effects on critical flow velocity of fluid-conveying microtubes via nonlocal strain gradient theory, *Microfluidics and Nanofluidics* **20**(5): 1-12.
- [36] Li L., Li X., Hu Y., 2016, Free vibration analysis of nonlocal strain gradient beams made of functionally graded material, *International Journal of Engineering Science* **102**: 77-92.
- [37] Şimşek M., 2016, Nonlinear free vibration of a functionally graded Nano beam using nonlocal strain gradient theory and a novel Hamiltonian approach, *International Journal of Engineering Science* **105**: 12-27.
- [38] Şimşek M., 2016, Axial vibration analysis of a nanorod embedded in elastic medium using nonlocal strain gradient theory, *Çukurova Üniversitesi Mühendislik-Mimarlık Fakültesi Dergisi* **31**(1): 213-221.
- [39] Tang Y., Liu Y., Zhao D., 2016, Viscoelastic wave propagation in the viscoelastic single walled carbon nanotubes based on nonlocal strain gradient theory, *Physica E: Low-dimensional Systems and Nanostructures* **84**: 202-208.
- [40] Fernandes R., 2017, Nonlinear size-dependent longitudinal vibration of carbon nanotubes embedded in an elastic medium, *Physica E: Low-dimensional Systems and Nanostructures* **88**: 18-25.
- [41] Shen Y., Chen Y., Li L., 2016, Torsion of a functionally graded material, *International Journal of Engineering Science* **109**: 14-28.
- [42] Guo S., 2016, Torsional vibration of carbon nanotube with axial velocity and velocity gradient effect, *International Journal of Mechanical Sciences* **119**: 88-96.
- [43] Li X., 2017, Bending, buckling and vibration of axially functionally graded beams based on nonlocal strain gradient theory, *Composite Structures* **165**: 250-265.
- [44] Li L., Hu Y., 2017, Post-buckling analysis of functionally graded Nano beam s incorporating nonlocal stress and microstructure-dependent strain gradient effects, *International Journal of Mechanical Sciences* **120**: 159-170.
- [45] Ebrahimi F., Barati M.R., Dabbagh A., 2016, A nonlocal strain gradient theory for wave propagation analysis in temperature-dependent inhomogeneous nanoplates, *International Journal of Engineering Science* **107**: 169-182.
- [46] Wang G.-F., Feng X.-Q., 2009, Surface effects on buckling of nanowires under uniaxial compression, *Applied Physics Letters* **94**(14): 141913.
- [47] Hosseini S.A.H., Rahmani O., 2016, Surface effects on buckling of double Nano beam system based on nonlocal timoshenko model, *International Journal of Structural Stability and Dynamics* **16**(10): 1550077.
- [48] He J., Lilley C.M., 2008, Surface effect on the elastic behavior of static bending nanowires, *Nano Letters* **8**(7): 1798-1802.
- [49] Farshi B., Assadi A., Alinia-ziazi A., 2010, Frequency analysis of nanotubes with consideration of surface effects, *Applied Physics Letters* **96**(9): 093105.
- [50] Abbasion S., 2009, Free vibration of microscaled Timoshenko beams, *Applied Physics Letters* **95**(14): 143122.
- [51] Ansari R., 2014, Nonlinear vibration analysis of Timoshenko Nano beam s based on surface stress elasticity theory, *European Journal of Mechanics - A/Solids* **45**: 143-152.
- [52] Lei X.-w., 2012, Surface effects on the vibrational frequency of double-walled carbon nanotubes using the nonlocal Timoshenko beam model, *Composites Part B: Engineering* **43**(1): 64-69.
- [53] Lee H.-L., Chang W.-J., 2010, Surface effects on frequency analysis of nanotubes using nonlocal Timoshenko beam theory, *Journal of Applied Physics* **108**(9): 093503.
- [54] Wang G.-F., Feng X.-Q., 2009, Timoshenko beam model for buckling and vibration of nanowires with surface effects, *Journal of Physics D: Applied Physics* **42**(15): 155411.
- [55] Arash B., Wang Q., 2012, A review on the application of nonlocal elastic models in modeling of carbon nanotubes and graphenes, *Computational Materials Science* **51**(1): 303-313.

- [56] Wang Q., Wang C.M., 2007, The constitutive relation and small scale parameter of nonlocal continuum mechanics for modelling carbon nanotubes, *Nanotechnology* **18**(7): 075702.
- [57] Younesian D., Nankali A., Motieyan E., 2011, Optimal nonlinear energy sinks in vibration mitigation of the beams traversed by successive moving loads, *Journal of Solid Mechanics* **3**(4): 323-331.
- [58] Rajabi K., Kargarnovin M., Gharini M., 2013, Dynamic analysis of a functionally graded simply supported Euler–Bernoulli beam subjected to a moving oscillator, *Acta Mechanica* **2013**: 1-22.
- [59] Pang M., Zhang Y.Q., Chen W.Q., 2015, Transverse wave propagation in viscoelastic single-walled carbon nanotubes with small scale and surface effects, *Journal of Applied Physics* **117**(2): 024305.
- [60] Naderi A., Saidi A., 2013, Modified nonlocal mindlin plate theory for buckling analysis of nanoplates, *Journal of Nanomechanics and Micromechanics* **4**(4): A4013015.
- [61] Shenoy V.B., 2005, Atomistic calculations of elastic properties of metallic fcc crystal surfaces, *Physical Review B* **71**(9): 094104.